

A genetic mouse model recapitulates immune checkpoint inhibitor-associated myocarditis and supports a mechanism-based therapeutic intervention

Spencer C. Wei^{1*}, Wouter C. Meijers^{2*}, Margaret L. Axelrod², Nana-Ama A.S. Anang¹, Elles M. Screever², Elizabeth Brunner Wescott⁴, Douglas B. Johnson², Elizabeth M. Whitley³, Lorenz Lehmann⁶, Pierre-Yves Courand⁷, James J. Mancuso¹, Lauren E. Himmel⁴, Benedicte Lebrun-Vignes¹³, Matthew J. Wleklinski², Bjorn C. Knollmann², Jayashree Srinivasan⁵, Yu Li⁵, Oluwatomisin T. Atolagbe¹, Xiayu Rao⁸, Yang Zhao⁸, Jing Wang⁸, Lauren Ehrlich^{5,9}, Padmanee Sharma^{10,11}, Joe-Elie Salem^{2,12}, Justin M. Balko^{2,4}, Javid J. Moslehi^{2, #}, and James P. Allison^{1, 11, #}

Supplemental Material

2 tables

10 figures

Supplemental Tables:

	<i>Ctla4^{+/-} Pdc1^{-/-} mice</i>		<i>Ctla4^{+/+} Pdc1^{-/-} mice</i>	
Heart				
<i>Number of mice evaluated</i>	54		59	
<i>Percentage male</i>	48%		56%	
<i>Percentage female</i>	52%		44%	
<i>Mean age evaluated</i>	154.5 days		164.4 days	
	Male	Female	Male	Female
<i>Percentage of mice with lymphocytic infiltrate</i>	23%	39%	0.09%	19%
<i>Mean lymphocytic infiltrate histology score</i>	2.46	3.71	0.76	1.23
<i>Percentage of mice with T cell infiltrate</i>	34.6%	42.9%	15.2%	19.2%
<i>Mean T cell infiltrate score</i>	3.04	5.73	1.59	2.36
Pancreas				
<i>Number of mice evaluated</i>	44		42	
<i>Percentage male</i>	48%		45%	
<i>Percentage female</i>	52%		55%	
<i>Mean age evaluated</i>	139.6 days		149.4 days	
	Male	Female	Male	Female
<i>Percentage of mice with lymphocytic infiltrate</i>	71%	87%	11%	30%
<i>Mean lymphocytic infiltrate histology score</i>	4.43	5.13	0.68	1.13
<i>Percentage of mice with T cell infiltrate</i>	62%	77%	39%	43%
<i>Mean T cell infiltrate score</i>	3.15	3.27	1.22	1.52
<i>Percentage of mice with exocrine atrophy</i>	43%	57%	5%	0%

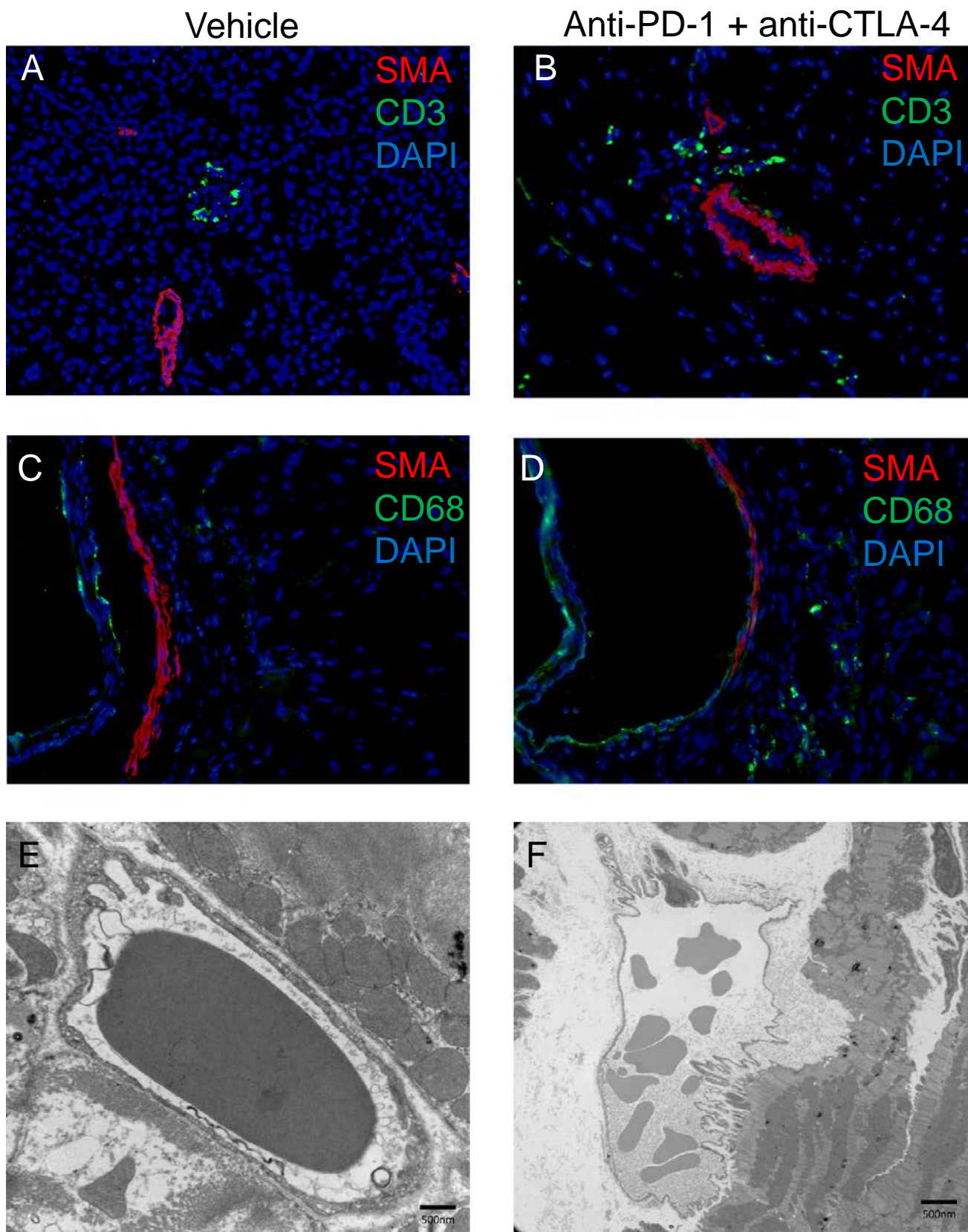
Supplemental Table 1. Histological analyses of heart and pancreatic tissues of *Ctla4^{+/-} Pdc1^{-/-}* mice and *Ctla4^{+/+} Pdc1^{-/-}* mice.

Semi-quantitative histologic scores of heart and pancreatic tissues. Mouse characteristics including age, sex, and genotype are denoted. Lymphocytic infiltration was defined by a histologic score of greater or equal to 2 of H&E stained tissue section (see Methods). T cell infiltrate was defined by a histologic score of greater or equal to 2 for CD3 IHC stained tissue sections.

Demog	Cancer Medical History	ICI regimen; number of doses received	Time to onset myocarditis; concurrent irAE	Myocarditis presentation	Immuno-modulators and other support (treatment sequence)	Outcome
66y, F, 50kg	- Treated for metastatic lung cancer (1 st line: carboplatin, pemetrexed) - Past history of thymoma (surgery and chest Rx 20 years earlier) complicated paralysis of diaphragm	2 nd line: Nivolumab (240 mg/2 weeks); 3 doses	37 days; myositis, hepatitis, arthritis (flare), myasthenia gravis like	Pseudo-ST+ (cMRI +, normal cAngio); Max Trop-T: 6.2 _{ng/ml} ; Max NTpro-BNP: 6.8 _{ng/ml} ; Min LVEF (55%); PVC (10-14,000/day with triplets); compatible ICI-irAE peripheral muscle biopsy	1/ Corticoreistant (3 days of 500mg IV MP) 2/ Plasmapheresis resistant (5 sessions) 3/ Abatacept (500mg IV/2weeks, 5 doses) plus steroids (1mg/kg/day PO prednisone with 5mg/2weeks tapering)	- Progressive normalization of biomarkers of myositis, hepatitis, myocarditis - Complete resolution of PVCs, LVEF remained normal - Discharge home at 1.5 month (stable cancer disease) - Died home at 3.5 months (care refusal, respiratory distress: pulmonary infection and embolism)
71y, M, 70 kg	- Treated for metastatic prostate cancer (previous lines: docetaxel, abiraterone and bone Rx)	Pembrolizumab (200 mg/3 weeks); 2 doses	33 days; myositis; hepatitis; arthritis, myasthenia gravis like	Initial myositis presentation complicated after one week by a complete atrio-ventricular block (cAngio with no significant coronary artery stenosis); Max Trop-I: 1.7 _{ng/ml} ; Max NTproBNP 0.83 _{ng/ml} ; Min LVEF (60%); non-sustained ventricular tachycardia; compatible ICI-irAE peripheral muscle biopsy	1/ Oral prednisone 1mg/kg/day during 1 week for myositis treatment 2/ 3 days of 1000mg IV MP when myocarditis was suspected (complete atrio-ventricular block) 3/ Abatacept 500 mg IV / 2weeks, 3 doses) plus steroids (1 mg/kg/day PO prednisone) with a progressive tapering over 3 months	- Progressive normalization of Trop-I at 3 weeks with a major decreased 24 hours after the first abatacept dose of (0.4 _{ng/ml}) - complete resolution of ventricular arrhythmia after abatacept - LVEF remained normal - Hospital discharge at day 43 - Alive with stable cancer disease at 4 months, tentative new line (enzalutamide)
68y, F, 63kg	- Treated for thymus carcinoma (previous lines: carboplatine, paclitaxel) - Past history of breast cancer (surgery and radiation 28 and 9 years ago)	Pembrolizumab (200mg/3 weeks); 1 dose	21 days; Myositis; Myasthenia gravis like syndrome	Primarily muscle pain, diplopia, fatigue. Then dyspnea (NYHA II-III). InitialTnT: 0.52 ng/ml, max. 3.7 ng/ml. Max. NT-proBNP: 5.6 ng/ml, CK: 6288 U/l. ST-elevations in I,II,III, aVF, V4-V6. Min. LVEF 45%, cMRI+, biopsy+	1000mg prednisone i.v. for 1 day, 500mg for 2 days, 250mg for 3 days; IgG immunoglobulines (2x, day 5-6), plasmapheresis (5x, day 8-12), Abatacept 500mg (5x, every 2 weeks, beginning day 13) with steroid tapering	- Progressive normalization of biomarkers of myositis and myocarditis after Abatacept treatment - LVEF normalization - Tracheotomy with long term ventilation for 2 month - Covered LV rupture, after 3 month - Alive with stable cancer disease 6 month after initial myocarditis

Supplemental Table 2. Case series of patients with ICI-associated myocarditis treated with abatacept

Supplemental Figure 1

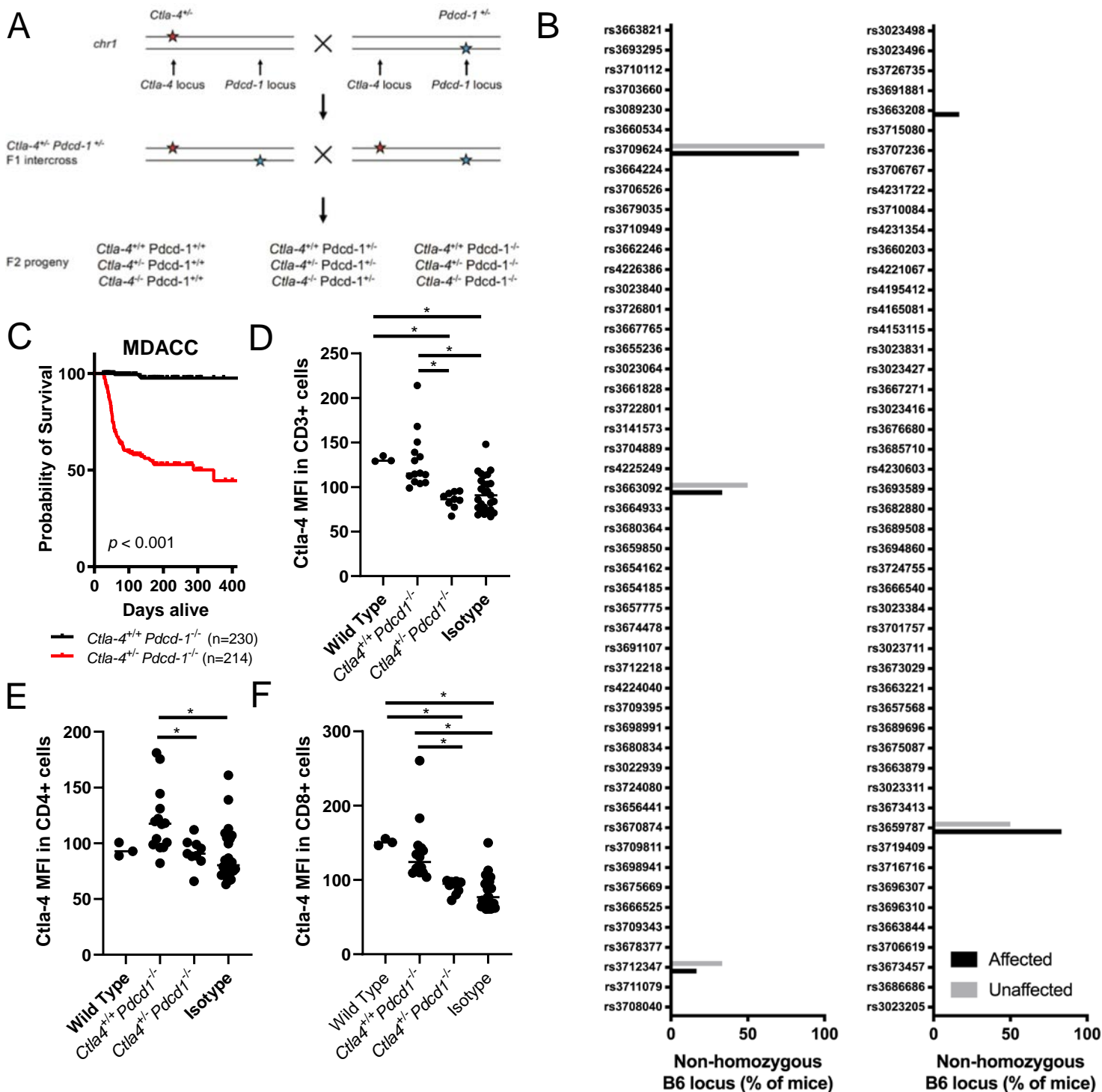


Supplemental Figure 1: Pharmacological inhibition of CTLA-4 and PD-1 leads to increased cardiac immune infiltration in MRL-*Fas*^{lpr} mice.

A-D) Immunofluorescent staining of cardiac tissue from MRL-*Fas*^{lpr} mice treated with vehicle or checkpoint blockade therapy.

E-F) Electron microscopy (EM) images of cardiac tissue from MRL-*Fas*^{lpr} mice treated with vehicle or checkpoint blockade therapy.

Supplemental Figure 2



Supplemental Figure 2: Generation and characterization transgenic mice with compound loss of function alleles of *Ctla4* and *Pdcd1*.

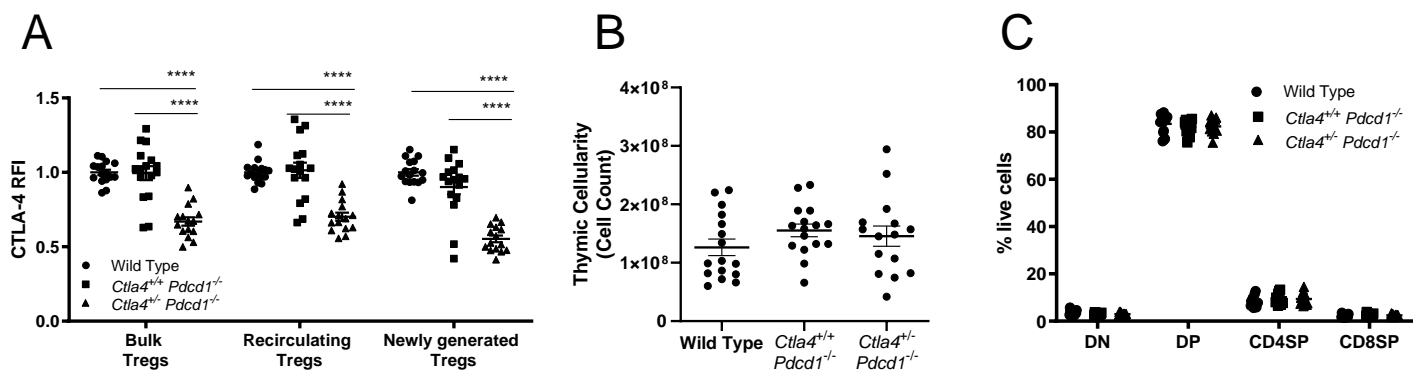
A) Schematic of the breeding scheme to generate all potential combinations of *Ctla4* and *Pdcd1* loss of function mutant alleles.

B) 100-SNP panel assessing strain background of *Ctla4*^{+/-} *Pdcd1*^{-/-} mice displaying clinical signs (affected) and not displaying clinical signs (unaffected). All tested mice harbored 96.5-100% C57BL6/J alleles. Non-homozygous B6 locus is defined as either heterozygous for B6/129 or homozygous for 129 alleles.

C) Kaplan-Meier survival curve of *Ctla4*^{+/-} *Pdcd1*^{-/-} ($n = 350$) and littermate *Ctla4*^{+/-} *Pdcd1*^{-/-} ($n = 400$) mice derived from a *Ctla4*^{+/-} *Pdcd1*^{-/-} by *Ctla4*^{+/-} *Pdcd1*^{-/-} breeding cross performed at the MD Anderson Cancer Center (MDACC) vivarium. P-value represents the result of the Mantel-Cox Log-rank test.

D-F) Total CTLA-4 protein levels in in vitro stimulated T cells from *Ctla4*^{+/-} *Pdcd1*^{-/-} and *Ctla4*^{+/-} *Pdcd1*^{-/-} mice lymph nodes. Mean fluorescence intensity (MFI) is displayed on a per mouse basis with mean and standard deviation. Isotype control stained samples for all groups are displayed as well as expression in wild-type C57BL6/J mice. *, $p < 0.05$ ANOVA with Tukey's multiple testing correction.

Supplemental Figure 3



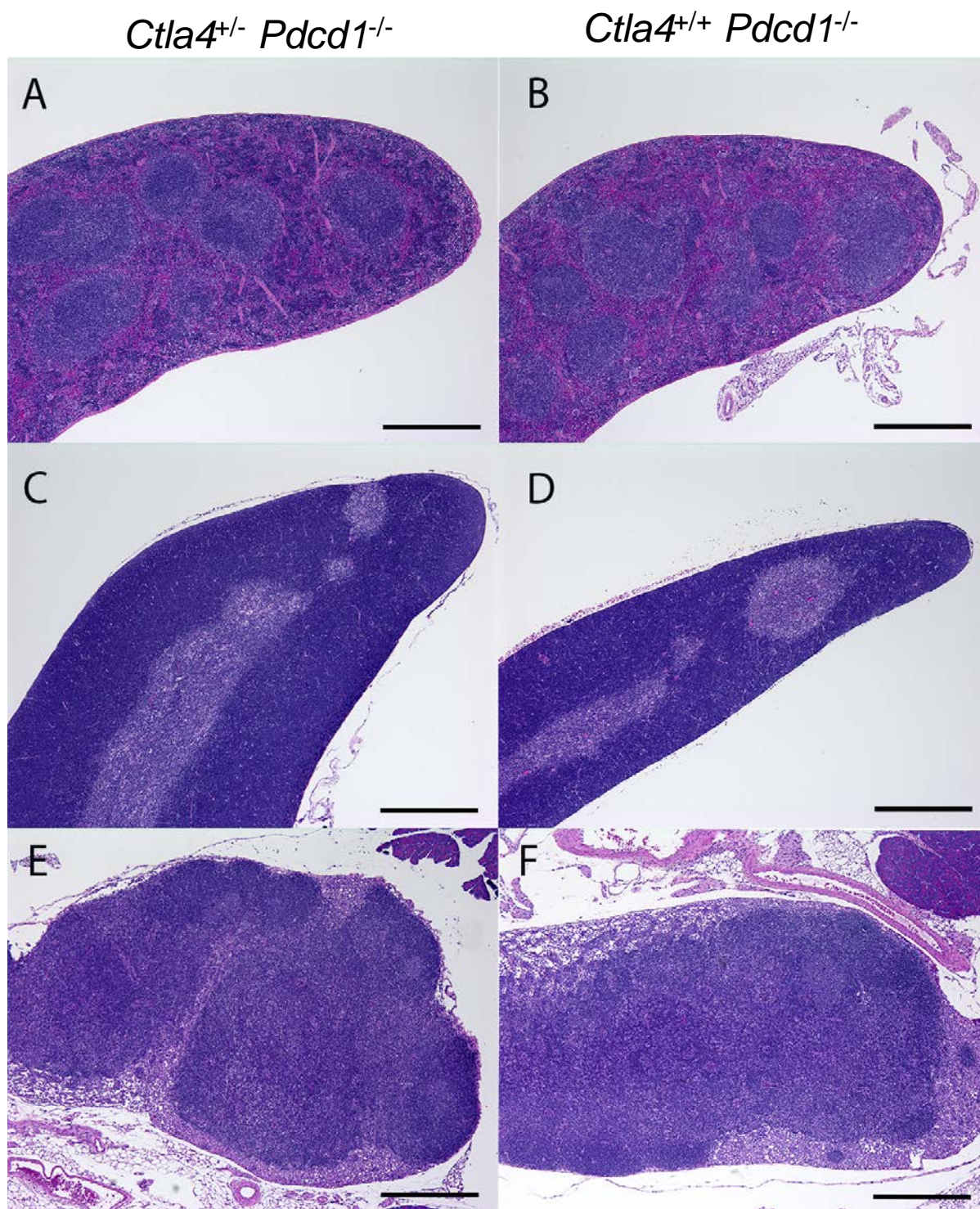
Supplemental Figure 3. Characterization of CTLA-4 expression and thymic development in *Ctla4^{+/-} Pcd1^{-/-}* mice.

A) Total CTLA-4 protein levels of thymus-derived T regulatory cells from wild-type C57BL6/J, *Ctla4^{+/-} Pcd1^{-/-}* and *Ctla4^{-/-} Pcd1^{-/-}* mice assessed by flow cytometry. Relative fluorescence intensity (RFI) is displayed on a per mouse basis with mean and standard deviation. Treg were identified as CD25⁺ FoxP3⁺ cells with newly generated and recirculating Treg cells defined as CD24^{high} Cd44^{low} and CD24^{low} CD44^{high}, respectively. RFI Expression levels are calculated as relative fluorescent intensities, normalized to CTLA-4 expression in C57BL6/J mice. *, p < 0.05 ANOVA with Tukey's multiple testing correction.

B) Thymic cellularity of wild-type C57BL6/J, *Ctla4^{+/-} Pcd1^{-/-}* and *Ctla4^{-/-} Pcd1^{-/-}* mice assessed by flow cytometry.

C) Thymic composition of wild-type C57BL6/J, *Ctla4^{+/-} Pcd1^{-/-}* and *Ctla4^{-/-} Pcd1^{-/-}* mice assessed by flow cytometry. CD4⁺ CD8⁻ double negative (DN), CD4⁻ CD8⁻ double positive (DP), CD4⁺ single positive (CD4SP), and CD8⁺ single positive (CD8SP)

Supplemental Figure 4



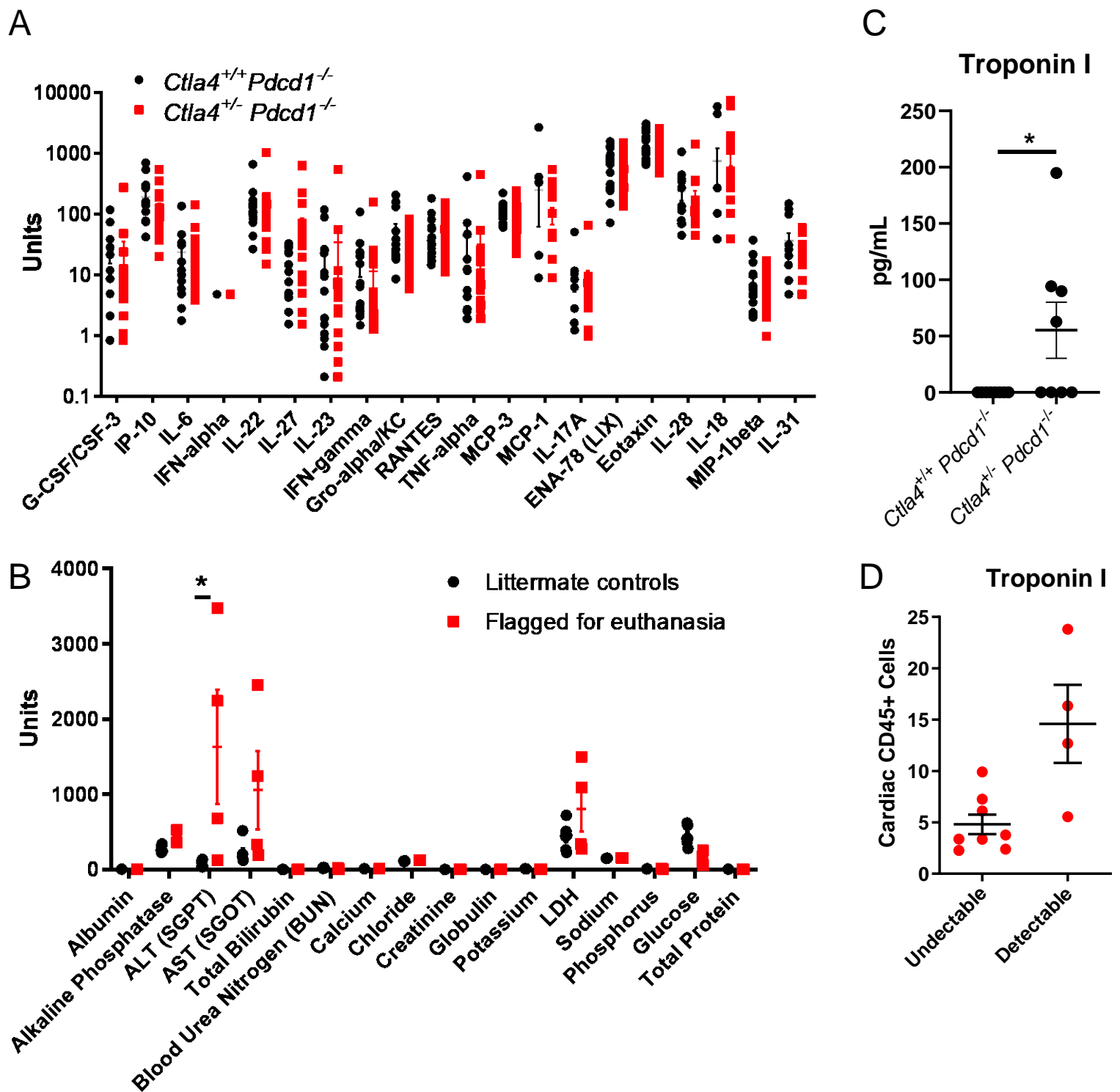
Supplemental Figure 4: Absence of lymphoproliferative or abnormal morphology in lymphoid tissues of *Ctla4^{+/-} Pdc1^{-/-}* mice.

A-B) Representative photomicrograph images of H&E stained spleen tissue from 28-day old *Ctla4^{+/-} Pdc1^{-/-}* and *Ctla4^{+/-} Pdc1^{+/-}* mice. Bar = 500 microns.

C-D) Representative photomicrograph images of H&E stained thymus tissue from 28-day old *Ctla4^{+/-} Pdc1^{-/-}* and *Ctla4^{+/-} Pdc1^{+/-}* mice. Bar = 500 microns.

E-F) Representative photomicrograph images of H&E stained mesenteric lymph node tissue from 28-day old *Ctla4^{+/-} Pdc1^{-/-}* and *Ctla4^{+/-} Pdc1^{+/-}* mice. Bar = 500 microns.

Supplemental Figure 5



Supplemental Figure 5. Characterization of serum properties in *Ctla4^{+/-} Pcd1^{-/-}* mice.

A) Serum levels of cytokine in *Ctla4^{+/-} Pcd1^{-/-}* and *Ctla4^{+/+} Pcd1^{-/-}* mice. Mice analyzed were 29-362 days old. This combined two cohorts, including a young cohort with *Ctla4^{+/-} Pcd1^{-/-}* mice that displayed clinical signs as well as aged mice. All comparisons included aged matched littermate controls.

B) Serum chemistry of *Ctla4^{+/-} Pcd1^{-/-}* mice displaying clinical signs requiring euthanasia and control littermate mice. Mice analyzed were 40-50 days old.

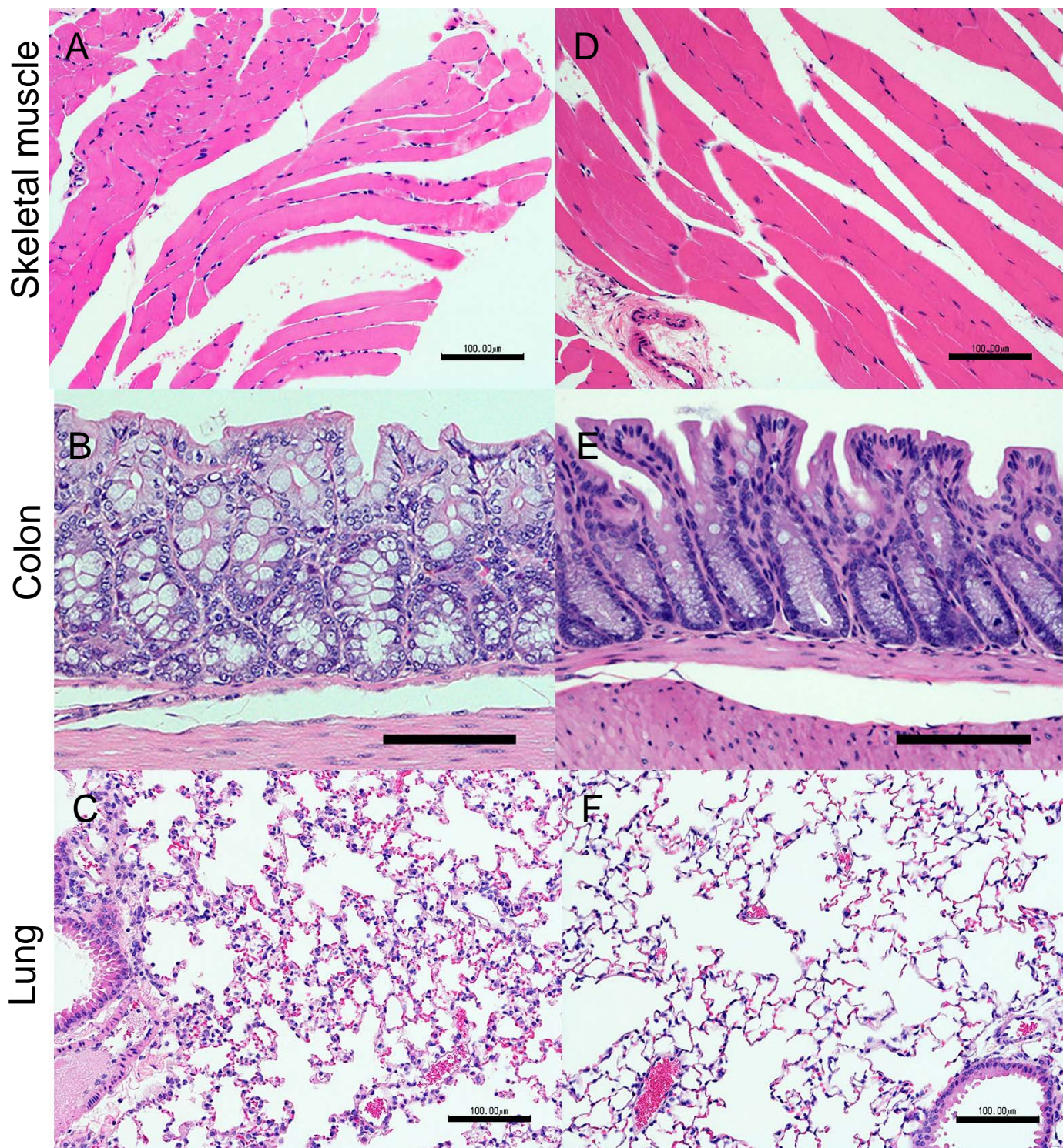
C) Serum troponin levels in *Ctla4^{+/-} Pcd1^{-/-}* and *Ctla4^{+/+} Pcd1^{-/-}* mice. Mice analyzed were 40-50 days old. *, P<0.05 T-test with multiple testing correction.

D) CD45+ heart infiltration in *Ctla4^{+/-} Pcd1^{-/-}* mice where serum troponin levels were detectable via ELISA vs. those where they were not.

Supplemental Figure 6

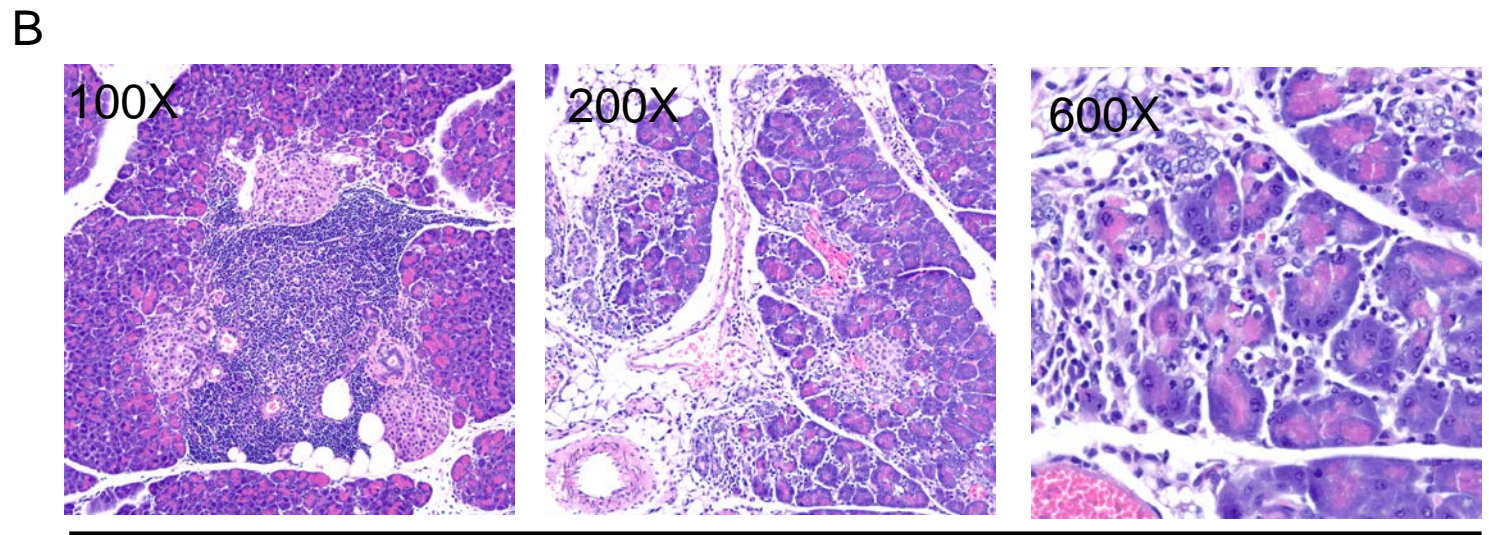
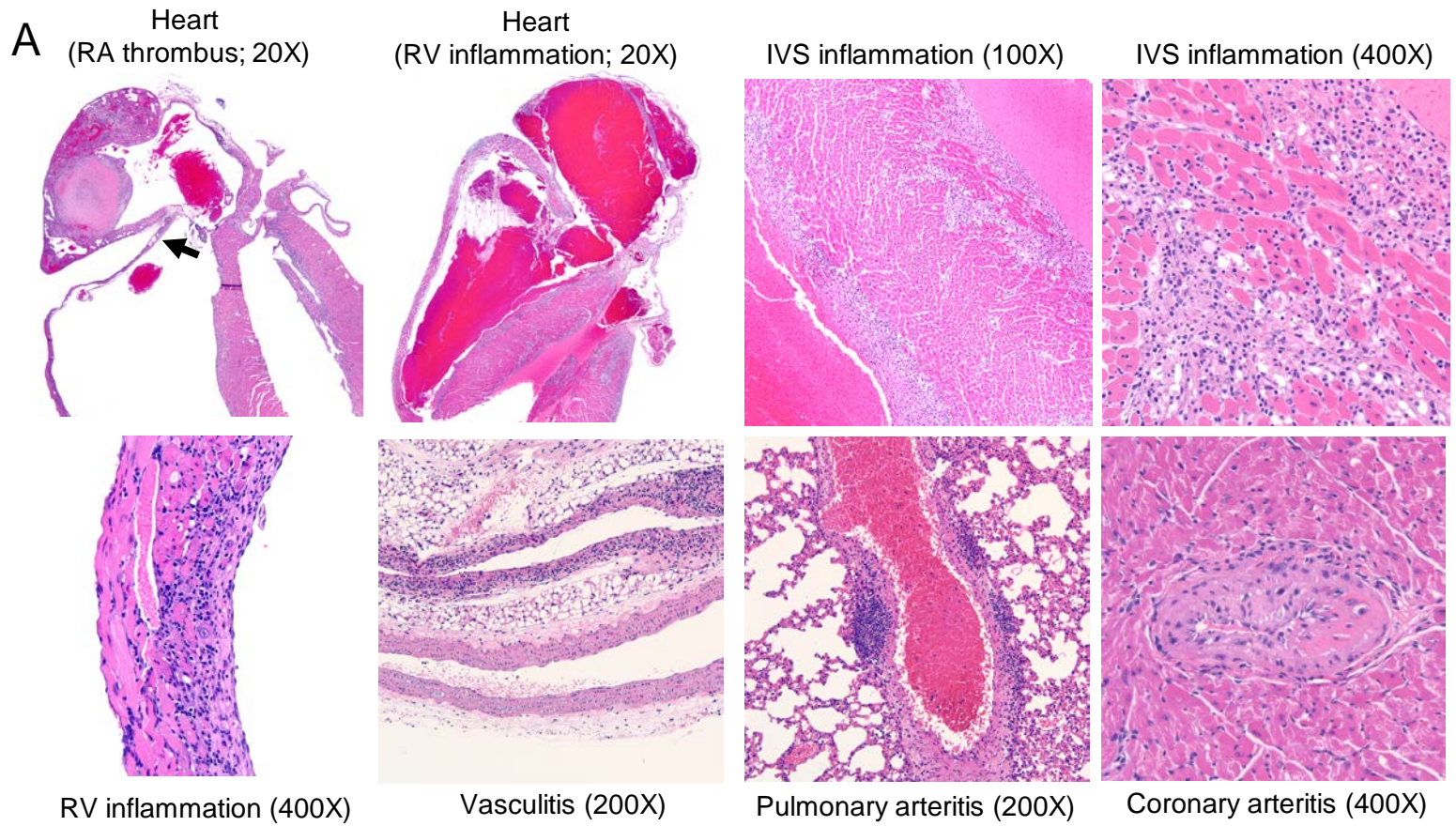
Ctla4^{+/-} *Pdcd1*^{-/-}

Ctla4^{+/+} *Pdcd1*^{-/-}

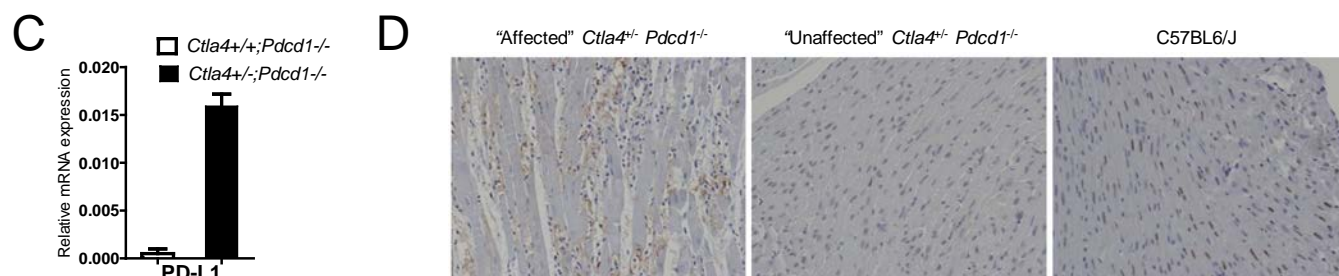


Supplemental Figure 6: Histopathology of skeletal muscle, colon and lung tissue in *Ctla4*^{+/-} *Pdcd1*^{-/-} mice. Representative photomicrographs of skeletal muscle, colon, and lung from littermate 99-day-old, male heterozygous (A, B, C) and wild-type (D, E, F) *Ctla-4* mice. Note the increased cellularity of the interstitium in the lung of the heterozygous mouse. Cellular infiltrates are not increased in skeletal muscle or colon, compared with the wild-type mouse (difference in degree of mucus distension of colonic goblet cells in the heterozygote is likely due to regional location of sample collection or secondary effects of *Ctla-4* deficiency.) Hematoxylin and eosin. Bar = 100 microns.

Supplemental Figure 7



Pancreas



Supplemental Figure 7. Cardiovascular and pancreatic histopathology in *Ctla4*^{+/-} *Pdc1*^{-/-} mice.

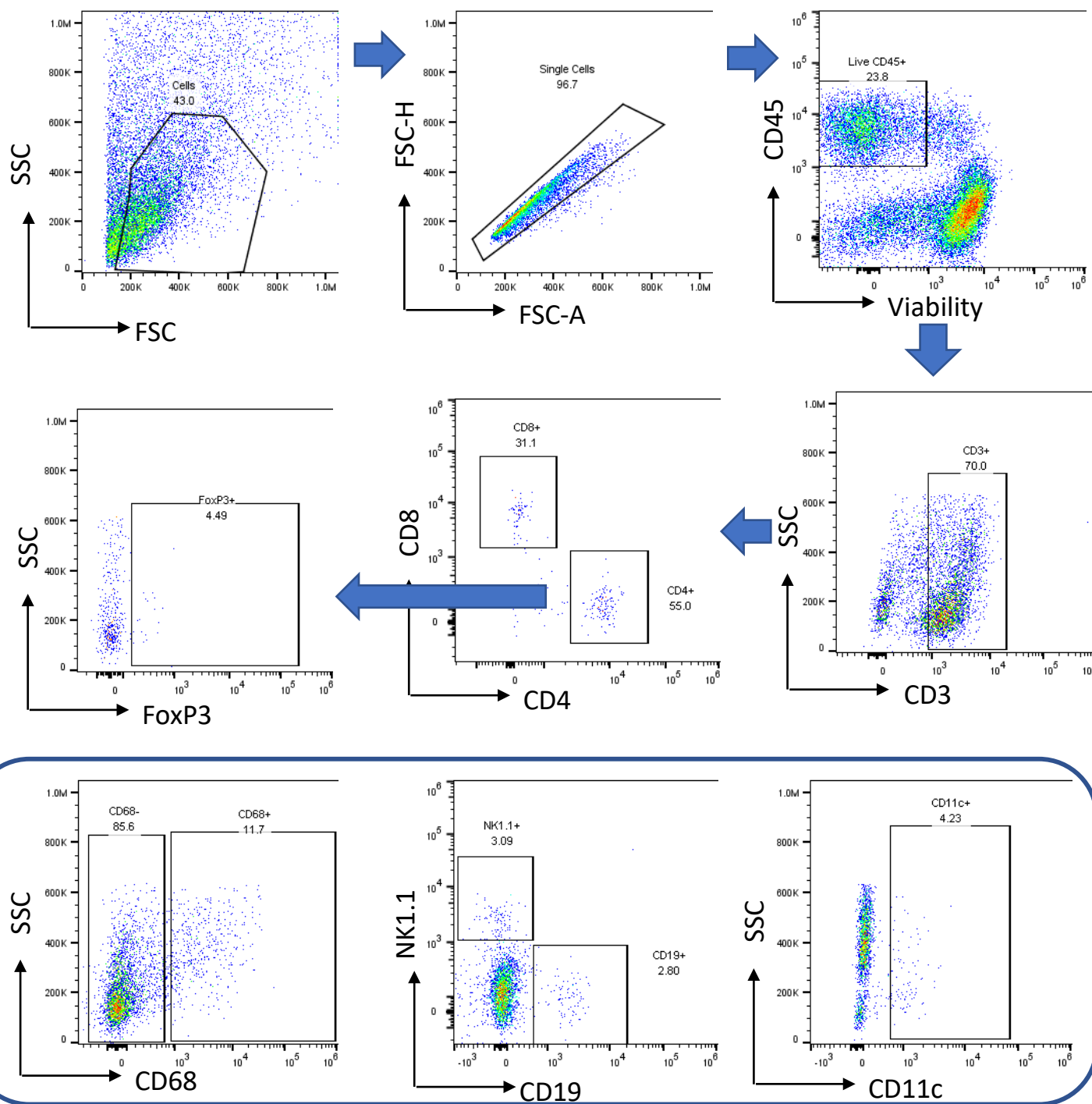
A) Photomicrograph images of H&E stained heart tissue from *Ctla4*^{+/-} *Pdc1*^{-/-} mice.

B) Photomicrograph images of H&E stained pancreatic tissue from *Ctla4*^{+/-} *Pdc1*^{-/-} mice

C) PD-L1 mRNA expression in cardiac tissue assessed by qPCR.

D) Example of PD-L1 expression assessed by immunohistochemistry in cardiac tissue in "affected" *Ctla4*^{+/-} *Pdc1*^{-/-} mice (displaying clinical signs), "unaffected" *Ctla4*^{+/-} *Pdc1*^{-/-} mice, and C57BL6/J wild-type mice for reference.

Supplemental Figure 8

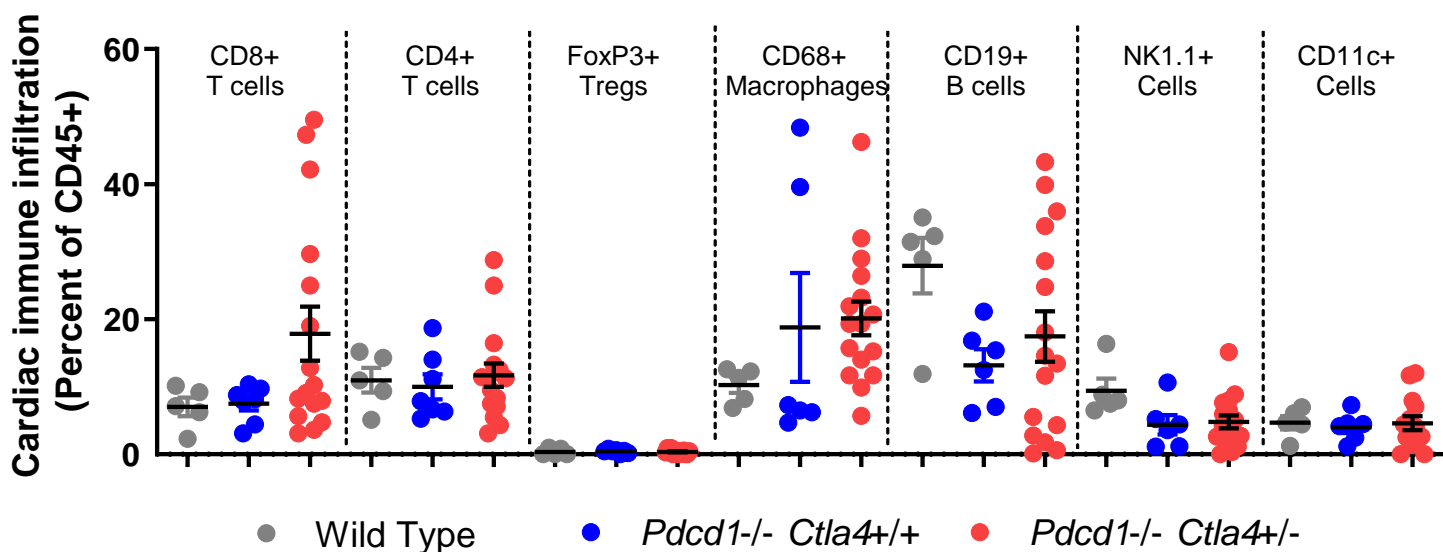


Supplemental Figure 8: Gating strategy/example for characterization of cardiac immune infiltrates *Ctla4^{-/-} Pcd1^{-/-}* mice.

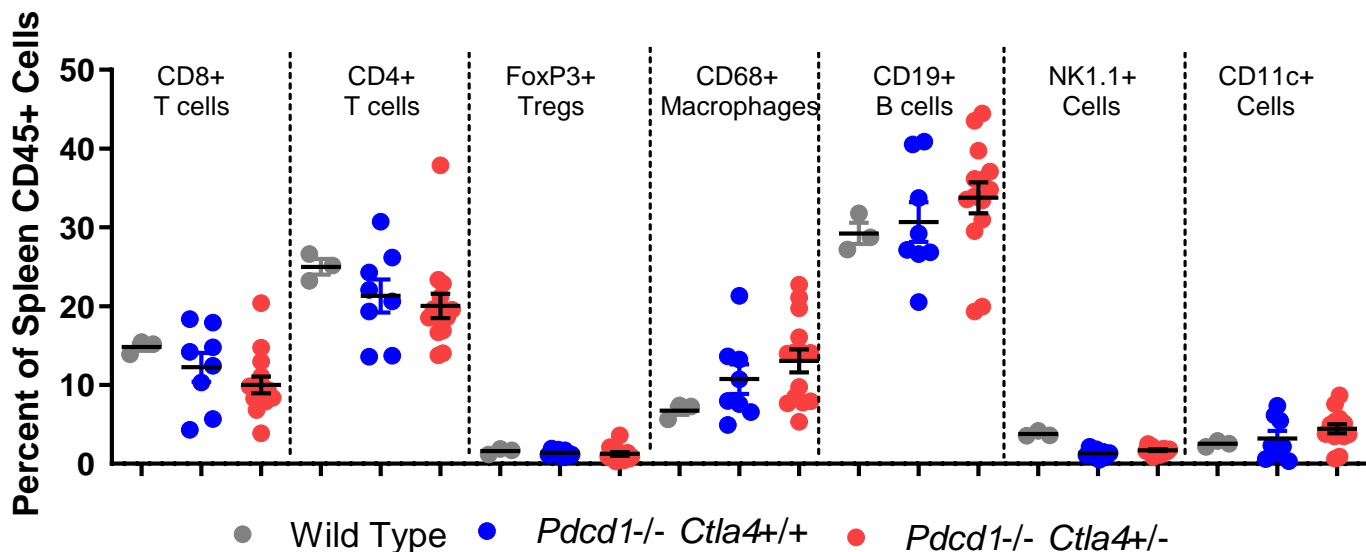
Dissociated cardiac tissue from mice were gated for singlet status, viability, and CD45 positivity, followed by enumeration of the identified populations.

Supplemental Figure 9

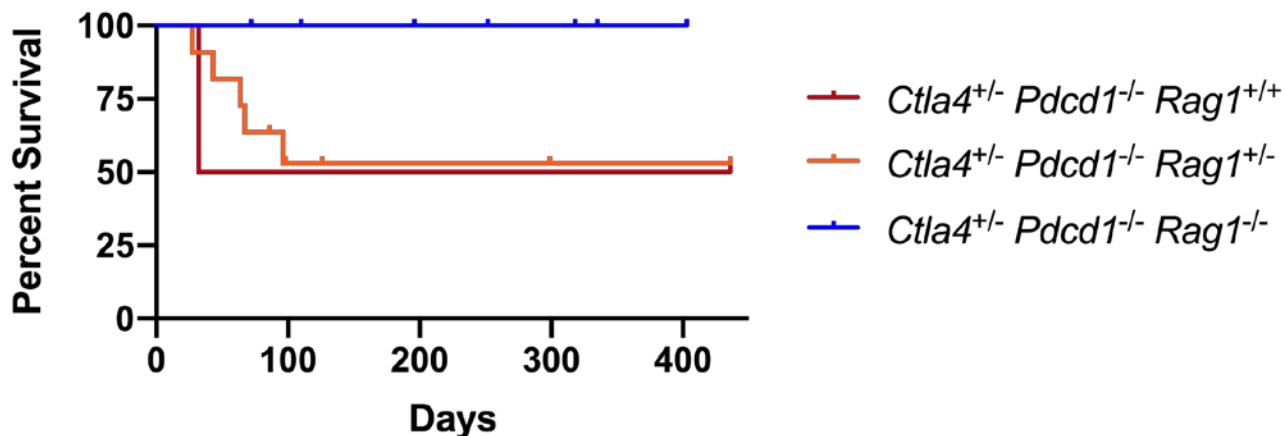
A



B



C

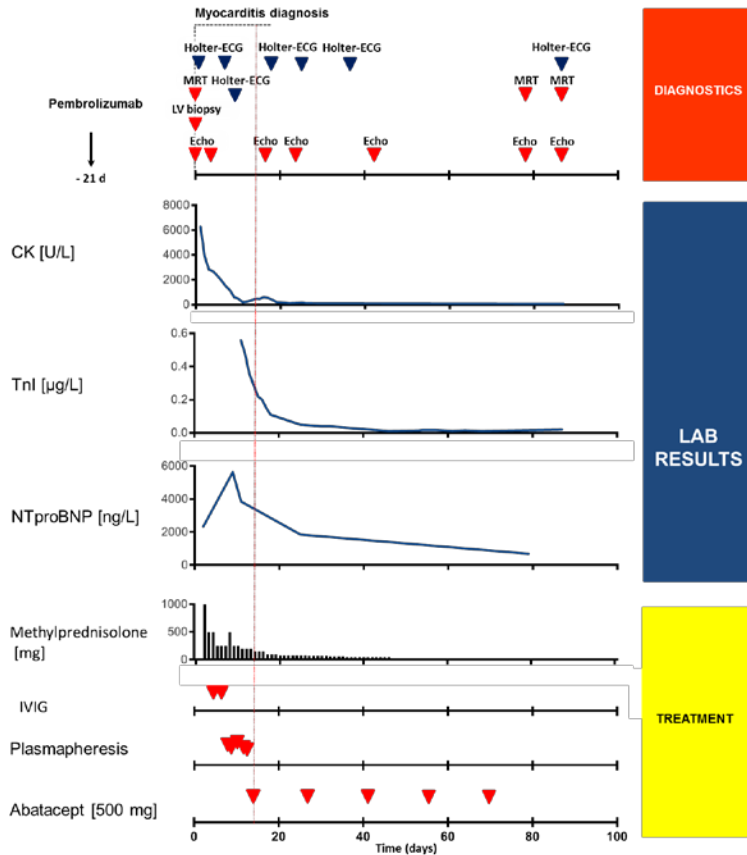


Supplemental Figure 9: Characterization of splenic populations among genotypes and survival analysis of female *Ctl4*^{+/-} *Pdc1*^{-/-} *Rag1*^{-/-} mice.

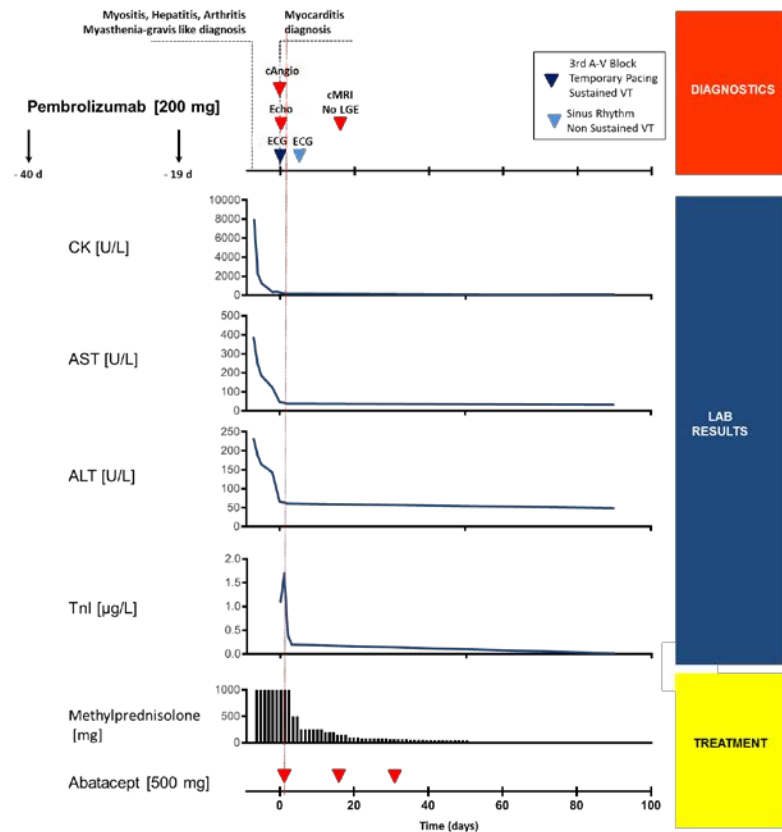
- A) Flow cytometry analysis of cardiac immune populations expressed as a percent of total CD45+ cells (No statistically significant different between groups by ANOVA)
- B) Flow cytometry analysis of immune populations in murine spleens, matched from Fig. 2E No statistically significant different between groups by ANOVA)
- C) Kaplan-Meier survival curve of female *Ctl4*^{+/-} *Pdc1*^{-/-} *Rag1*^{-/-} (n=7) and littermate female *Ctl4*^{+/-} *Pdc1*^{-/-} *RAG1* competent mice (n=11 and 2 for *Rag1*^{+/-} and *Rag1*^{+/+}, respectively).

Supplemental Figure 10

Patient 1



Patient 2



Supplemental Figure 10: Clinical course, diagnostic labs, and therapy in 2 immune-related myocarditis patients treated with abatacept